Effect of Graphene Oxide Synthesis Method on The Adsorption Performance of Pharmaceutical Contaminants

Mohd Faizul Idham
Water and Environment Engineering Laboratory, Interdisciplinary Graduate School of Engineering Sciences, Kyushu University

Falyouna, Omar
Water and Environment Engineering Laboratory, Interdisciplinary Graduate School of Engineering Sciences, Kyushu University

Eljamal, Osama
Water and Environment Engineering Laboratory, Interdisciplinary Graduate School of Engineering Sciences, Kyushu University

https://doi.org/10.5109/4738593

出版情報：Proceedings of International Exchange and Innovation Conference on Engineering & Sciences (IEICES). 7, pp.232-239, 2021-10-21. Interdisciplinary Graduate School of Engineering Sciences, Kyushu University
バージョン：
権利関係：

Effect of Graphene Oxide Synthesis Method on The Adsorption Performance of Pharmaceutical Contaminants

Mohd Faizul Idham[1,2], Omar Falyouna[1], Osama Eljamal[1*]
[1]Water and Environment Engineering Laboratory, Interdisciplinary Graduate School of Engineering Sciences, Kyushu University, 6-1 Kasuga-Koen, Kasuga, Fukuoka, Japan, 816-8580,
[2]School of Mechanical Engineering, College of Engineering, Universiti Teknologi MARA, Cawangan Terengganu
[*]Corresponding author email: osama-eljamal@kyudai.jp

Abstract: *Graphene oxide (GO) has drawn broad recognition as a novel adsorbent for various contaminants due to the unique physicochemical characteristics shown. This research investigated the effect of several graphene oxide synthesis methods on Ciprofloxacin (CIP), Diclofenac (DCF), and Tetracycline (TC) removal in water and optimized the methods experimentally. Material characterizations such as transmission electron microscopy (TEM) and energy-dispersive spectroscopy (EDS) were employed to investigate the surface morphology of GO. A batch test has been done to study the adsorption kinetics. GO synthesis techniques are crucial and have varying impacts on pharmaceutical contaminants removal. The optimized GO synthesis method showed the most reliable CIP removal performance, where 64% of CIP was effectively adsorbed within 10 minutes. The production of high-quality GO for CIP and DCF removal does not rely on sodium nitrate (NaNO3) or phosphoric acid (H3PO4) catalysts. The GO produced without catalysts eliminated 94.3% of DCF within 10 minutes.*

Keywords: Graphene Oxide; Water and wastewater treatment; Pharmaceutical Contaminants

1. INTRODUCTION

Water is an essential fundamental component of all life and a valuable resource for human amenities. Seventy percent of the human body is water, and water is required by the body to regulate body temperature and supply nutrients to the body's organs [1], [2]. Therefore, humans and even other creatures also need to consume a certain amount of water to sustain their life. In addition, water is a suitable and most efficient solvent for a wide range of mineral and organic compounds [3].

Although the standard of living of the global population today is rising, the lack of access to safe and drinkable water remains one of the most severe challenges and crises confronting the community worldwide [4]. Water pollution is one of the most pressing challenges facing the globe today as it will threaten ecosystems and poses health risks to human life through water-related diseases [5]–[7].

Generally, the community water systems are obtained from two sources, namely surface water and groundwater. The presence of contaminants such as toxic heavy metal ions and pharmaceutical contaminants in these water sources can be catastrophic to health [8]–[11]. Water contamination stems from various factors, including naturally occurring chemicals such as arsenic [12], radon, and uranium[13], besides agricultural practices such as fertilizers and pesticides [14]. Contamination problems are exacerbated by human related-activities such as industrial activities, manufacturing processes, sewer overflows, or wastewater discharges [15].

Conscious that water pollution requires appropriate treatment to eliminate disease-causing contaminants, appropriate measures or techniques have been developed for this purpose [16], [17]. Adsorption has proved to be one of the most practical, relatively fast, and cost-effective methods among the techniques available currently for removing contaminants from water [9][18] [19]. Thus numerous materials, including mesoporous materials [20], clay minerals [21], activated carbon [22], [23], zeolites [24], [25], nano-zero valent iron (nZVI)[18], [26] and polymers [27], [28], have been preferred to be used as adsorbents in water and wastewater treatment studies.

GO is one of the preeminent carbon nanomaterials that has generated global interest and attention in recent years. It has become desirable among environmentalists worldwide due to its excellent adsorption ability, remarkable mechanical strength, numerous functional groups, and large surface area [29], [30]. In comparison to other nanomaterials, GO exhibits different biochemical characteristics with low cytotoxicity [31], [32]. GO is oxidized graphene that has been functionalized with various responsive oxygenous functional groups [33]. It is typically synthesized through chemically graphite oxidation, producing in extended graphene sheets finished with carboxylic acid groups at the edges, including hydroxyl and epoxy functional groups in the basal planes [29], [34], [35]. These functional groups contribute significantly to high negative charge density and GO hydrophilicity properties [36], [37]. GO composites, in particular, have a significant advantage in removing different heavy metal ions, dyes, and pharmaceutical contaminants from water through adsorption [24], [38]–[40].

Nowadays, chemical techniques have become the most common methods for massive GO synthesis, including oxidation, exfoliation, and reduction levels. Graphite is transformed into GO by chemical synergies with solid acids such as sulphuric acid (H_2SO_4) and oxidizing agents [41]. The graphene is then synthesized from graphite as a raw material by a chemical or physical approach like thermal, chemical, mechanical, and electrochemical exfoliation [42], [43].

Researchers employed a variety of techniques and variations of substances to fabricate GO-based adsorbents for purifying contaminated water [40], [44]. The most widely reported technique for GO production is the Hummer method. Some researchers modified this

Hummer method by combining elements used to synthesize GO, such as H_3PO_4, H_2SO_4, and $NaNO_3$, in a certain amount for graphite oxidation. Apart from that, the variety of time ranges was also reported by most researchers to produce GO, and it was occasionally discovered that the creation procedure of this substance was time-consuming.

As far as the authors are concerned, there is limited information available regarding the influence of GO synthesis methods on the pharmaceutical contaminant removal performance by GO. Therefore this present study aims to study several GO synthesis methods on the performance of pharmaceutical contaminants removal in water and optimize the methods experimentally. The CIP, DCF, and TC adsorption capability of the synthesized GO was evaluated as quality measures.

2. MATERIALS AND METHODS

2.1 Materials

Graphite powder (particles size ~20 µm, purity >=99.5%), potassium permanganate ($KMnO_4$), H_2SO_4, H_3PO_4, Sodium Nitrate (NaNO3), hydrochloric acid (HCl), and hydrogen peroxide (H_2O_2) were acquired to synthesize the GO. In addition, the pharmaceuticals; Ciprofloxacin Hydrochloride ($C_{17}H_8FN_3O_3$•HCl•H_2O), Diclofenac Sodium Salt ($C_{14}H_{10}Cl_2NNaO_2$), and Tetracycline ($C_{22}H_{24}N_2O_8$-+XH_2O) were purchased from Tokyo Chemical Industry CO., LTD, Japan to prepare the pharmaceutical contaminant suspensions. Deionized water (DI) was employed in this work for the preparation of all the solutions. All the used materials were of analytical quality and were utilized in the tests without being modified or treated.

2.2 Synthesis of GO

In this present work, several GO synthesis methods have been selected from previous research and were studied for their effectiveness in removing pharmaceutical contaminants. Typically, the researchers introduced the modified Hummer method to synthesize the GO. The GO synthesis techniques were referenced in research [36], [33], and [43], giving three different GO samples, GOM1, GOM2, and GOM3, respectively. In general, all these methods use different parameters and chemical combinations.

Table 1 manifests the precise circumstances related to the parameters and materials used in synthesizing GO. This research classified the GO synthesis methods into six critical main threads: mixing I, oxidizing, mixing II, dilution-heating, dilution, and reducing. All these processes were run in a precise order and had a specific period. Mixing I is an essential initial process involving the main constituents of GO synthesis. First, graphite powder was mixed with concentrated H_2SO_4 and catalyst under vigorous stirring in an ice bath in this tread. Then, the suspension was held below 5°C before slowly adding $KMnO_4$ while stirring in the oxidizing process. Finally, the ice bath was withdrawn, and the further mixing (Mixing II) procedure began by heating the suspension to 35–38°C for a certain period. Next, the suspension was diluted with DI water and heated up for a specified duration to 95°C before being diluted with DI water at a temperature of 35°C unless stated otherwise. Following the dilution, the reducing process was carried out to stop the reaction and reduce the residual permanganate by adding a specific amount of 30% H_2O_2 to the suspension. It changed the suspension color to a brilliant yellow. The suspension was next centrifuged, and the precipitated product was washed with 30% HCl aqueous solution and DI water to remove soluble ions until the pH of the supernatant became neutral. The washed product was then dried for 24 hours at 60°C until it attained a consistent weight.

Pre-experiments were conducted on all these synthesized GOs to examine their performance in removing CIP. Then, an optimal method was derived based on the resulted performance for further investigation. It is emphasized here that the previously investigated GO synthesis techniques were simplified to optimize the method by eliminating and merging unnecessary steps, minimizing the number of chemicals used, and minimizing the total running time for the synthesis. Furthermore, mixing II periods in the GO synthesis optimized method on the CIP removal performance was also studied. Therefore, two GO samples were synthesized using the optimized method with mixing periods of 30 and 60 minutes, and both samples were designated as GO30 and GO60, respectively, in this paper.

The sonication technique was used to investigate its effect on CIP adsorption performance. In brief, the GO30 synthesis process was changed by including a sonication process for 30 minutes at 30°C following the mixing II stage. This sample was assigned as GO30-S30.

2.3 Characterization of GO

The GO samples' elemental compositions and high-resolution images were analyzed and taken using a JEOL JEM-2100F transmission electron microscope (TEM) with energy-dispersive spectroscopy (EDS). A micropipette was used to drop the specimen onto a carbonated copper grid plate after the sample was dispersed in ethanol.

2.4 Batch experiment: Kinetics adsorption

CIP, DCF, and TC were used to prepare standard stock solutions of pharmaceutical contaminants with a concentration of 100 mg/L. The removal efficiencies of these pharmaceutical contaminants by various as-synthesized GO adsorbents were investigated by adding GO flakes (25 mg) into a 100 mL of pharmaceutical contaminants aqueous solution. The mixtures were controlled at 25°C in sealed conical flasks using a 1000-rpm magnetic stirrer (RSH-6DN, As One Co., Japan)

Table 1. GO synthesis parameters and materials used.

PROCESS	PARAMETER /MATERIAL	SAMPLE				
		GOM1 [36]	**GOM2** [33]	**GOM3** [43]	**GO30**	**GO60**
MIXING I	Graphite (g)	0.5 g	3 g	5 g	1 g	1 g
	H_2SO_4 (mL)	50 mL	40 mL	115 mL	20 mL	20 mL
	Catalyst	-	10 mL H_3PO_4	2.5 g $NaNO_3$	-	-
	Ice Bath	√	√	√	√	√
	Stirring	√	√	√	√	√
	Period (Minutes)	-	-	30	-	-
OXIDIZING	Potassium Permanganate, $KMnO_4$ (g)	2 g	6 g	15 g	3 g	3 g
	Ice Bath	√	√	√	√	√
	Stirring	√	√	√	√	√
	Period (Minutes)	120 min	20 min	90 min	20 min	20 min
MIXING II	Temperature (ºC)	35 ºC	35 ºC	38 ºC	38 ºC	38 ºC
	Stirring	√	√	√	√	√
	Period (Minutes)	60 min	30 min	30 min	30 min	60 min
DILUTION-HEATING	Deionized Water	50 mL	50 mL	250 mL	50 mL	50 mL
	Temperature (ºC)	< 100 ºC	98 ºC	95 ºC	95 ºC	95 ºC
	Stirring	√	√	√	√	√
	Ice Bath	√	-	-	-	-
	Period (Minutes)	60 min	30 min	15 min	10 min	10 min
DILUTION	Deionized Water	150 mL	150 mL			
	Stirring	√	√			
	Temperature (ºC)	-	30 ºC			
	Stirring	√	√			
	Period (Minutes)	-	30 min			
REDUCING	30% Hydrogen Peroxide, H_2O_2 (mL)	10 mL	40 mL	15 mL	3 mL	3 mL

Sampling times for adsorption analysis were 10, 20, 30, 60, 90, 120, and 180 min, filtering through 0.25 μm membrane to determine the residual pharmaceutical contaminant concentration (pH = 6). CIP, DCF, and TC concentrations in the supernatants were then measured using a UV–vis absorption spectrophotometer at emission wavelengths of 275, 276, and 355 nm, respectively. Quantitative analysis of these three pharmaceutical drugs was performed using a UV-vis spectrophotometer (UV-1280, Shimadzu, Japan).

3. RESULTS AND DISCUSSIONS

3.1 Surface Morphology

The surface morphologies of GO synthesized using various methods were observed using TEM and are represented in Fig. 1. The images revealed that the graphite peeling was utterly compelling, with multiple GO layers forming, indicating that all methods employed in this research effectively transformed graphite to GO. There were no significant variations in any samples' surface morphology shown since the GO samples exhibit a typically wrinkled morphology and sheet-like structure due to oxygen-containing functional groups splicing on their surface [10], [33]. The synthesized monolayer GO sheets typically have a thickness of 0.7–1.2 nm [29]. Although the synthesis methods of GOM1, GO30, and GO60 did not use any catalyst to promote transforming graphite to GO, and even though the GO30, GO60, and GO30-S30 synthesis methods were shorter than other presented ways, these circumstances did not affect the graphite peeling process. On the other hand, vigorous stirring using a mechanical stirrer during the mixing process has assisted the graphite peeling process for these samples. The sheets on the graphite's structure generally accumulate on each other due to the weak Van der Waals forces [8], [38], [40]. Then the vigorous mechanical stirring process deforms the graphite sheets' structure, efficiently peeling graphite into the GO layers. The enlarged layers of graphite were eroded due to the microjets produced by the bubbles' burst during the process [42].

3.2 Elemental Analysis

The elemental compositions of synthesized GO were analyzed before adsorption experiments using energy-

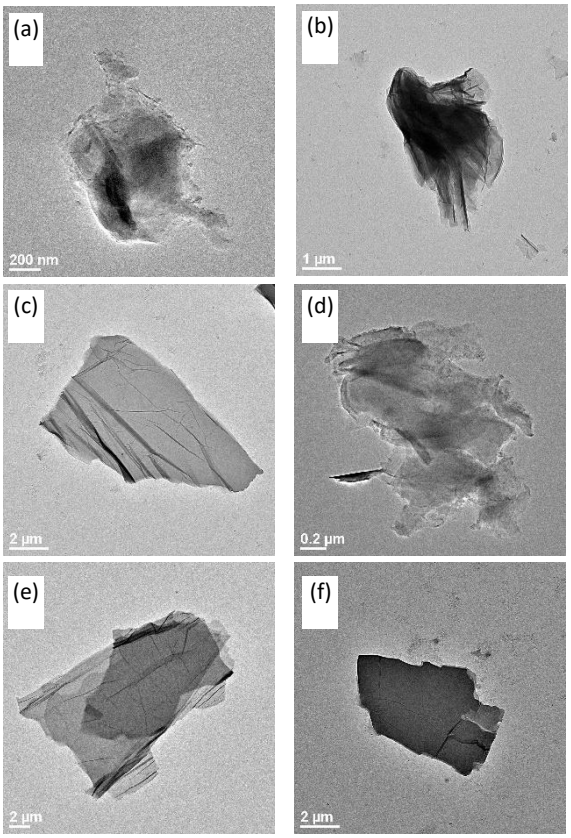

Fig. 1. TEM images. (a) GOM1; (b) GOM2 (c) GOM3; (d) GO30; (e) GO60; (f) GOS30;

dispersive spectroscopy (EDS) connected to the TEM instruments. Table 2 tabulates the elemental composition of GO samples, which contained carbon and oxygen atoms (wt.%). Khalil et al. [38] reported that graphite was almost entirely composed of carbon, with less than 1% oxygen. Since graphite is practically a non-oxidized material containing a tiny and negligible amount of oxygen, it can be considered to have a carbon content of 100% [16]. By comparing the oxygen content, GO samples show a higher amount of oxygen than graphite. These results confirmed that graphite was successfully transformed to GO for all samples. It also proved oxygen-containing functional groups (OCFGs) on GO, contributing to the enhanced removal efficiency of adsorption of pharmaceutical contaminants [11][38]. Almost all GO samples contained oxygen content of about 30% and higher except GOM1 and GO30. Both samples contained oxygen less than 10% because, during the oxidation process, no catalyst was employed in the synthesizing process. The use of catalyst materials such as H_3PO_4 and $NaNO_3$ has led to an increment of the oxygen content, as demonstrated by the samples GOM2 (29.62 wt.%) and GOM3 (34.30 wt.%). However, the oxygen content of the samples GO60 and GO30-S30 showed a high content of 38.72% and 30.38%, respectively, although the synthesis process did not rely on catalysts. These findings confirmed that the prolongation of the reaction time in the heating process could enhance the oxygen content without using any catalyst, besides proving that the sonication process has no substantial effect on the oxygen content of the material. Higher oxygen content indicates the high oxidation level of the GO sample [33].

Table 2. elemental compositions of synthesized GO samples

SAMPLES	C %	O %
GOM1	92.11	7.89
GOM2	70.38	29.62
GOM3	65.70	34.30
GO30	90.49	9.51
GO60	61.28	38.72
GO30-S30	69.62	30.38

3.3 Kinetics Adsorption: CIP

Initially, a batch test was performed on GOs synthesized using three different methods to determine the kinetic profile of the materials adsorbing CIP at various times interval, and the findings are represented in Fig. 2. Overall, a dramatic decline in CIP concentration demonstrates the rapid adsorption kinetics of all samples within the first 10 minutes. The fast adsorption kinetics shown by GO samples were due to the heterogeneous chemisorption. This reaction involved the interaction between functionalized GO's edges and the aromatic structure in the basal planes of GO to the two charged functional groups and the electro secondary π structure of CIP [37]. The GOM2 sample shows a slowly increased CIP removal trend over time, reaching a removal efficiency of 40% at a 3-hour interval. On the other hand, the adsorption process by the GOM1 sample reached equilibrium at the same removal efficiency in less than 90 minutes. Furthermore, the contaminant removal activity was more stable as there was no significant change in CIP concentration over the period. However, more significant CIP removal was observed with GOM3. It is found that 64% of CIP was removed from the contaminated water in the first 10 minutes, indicating more OCFG was induced on the surface of the synthesized GO supported by $NaNO_3$ to remove CIP. This finding is consistent with the elemental composition result showing significant oxygen content in this sample. The amount of OCFGs plays a crucial function in the CIP adsorption process [30]. Nevertheless, the fluctuation trend displayed by the graph indicates the nonequilibrium and instability of the material in CIP adsorption due to adsorption and desorption activities throughout the process. This phenomenon happens due to the weak electrostatic attraction between the adsorbent surface and cationic CIP, thus affecting the final CIP concentration at the respective period. These results show that the synthesis technique used to produce GO influences antibiotics' adsorption performance and removal properties. The application of H_3PO_4 as a catalyst to transform graphite to GO did not provide appropriate benefits as it reduced the CIP adsorption kinetics rate. While the use of $NaNO_3$ as a catalyst in the GO synthesis process enhanced the rate of CIP removal and the adsorption process became unstable.

These preliminary findings have driven the optimization of the GO synthesis method. Both optimized samples, GO30 and GO60, are shown to have significantly higher adsorption stability than GOM3 and higher CIP removal efficiency than GOM1 and GOM2. The strong

electrostatic interaction between cationic CIP species and carboxyl or phenol groups on GO, particularly at the edges, was responsible for the adsorption stability of these GO samples [39]. Despite that, GO30 and GO60 have shown no significant differences in CIP removal efficiency and adsorption stability, indicating the mixing II period during synthesis did not significantly impact GO performance in removing CIP. Faster adsorption kinetics was shown by the GO30 and GO60 samples when the CIP concentration dropped sharply in the first 10 minutes of the test, with the removal efficiency reaching 55.9% and 57%, respectively. The reaction can be considered to have achieved an equilibrium starting at 30 minutes, as there was no notable change in CIP concentration after this time. At 3 hours, both samples showed CIP removal efficiency reaching 60-61%, which was a higher value than that shown by GOM3.

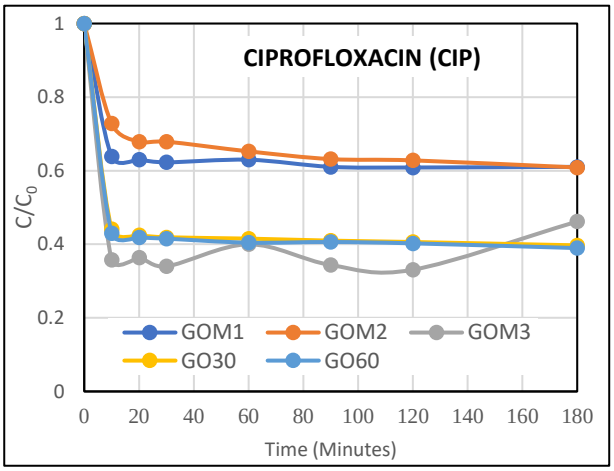

Fig. 2. Effect of contact time on adsorption of CIP

Arabpour et al. [42] found that the sonication step was essential in the GO synthesis procedure to remove Methylene Blue in their study. Therefore, the effect of the sonication step was also studied in this research to observe its effects on the GO quality for CIP removal. Fig. 3 depicts the difference in CIP adsorption kinetics on the GO30 sample and the GO sample synthesized by completing a 30-minutes sonication step (GO30-S30) at 30ºC. Both samples resulted in the identical CIP removal efficiency of 55.9% through the first 10 minutes. After 3 hours, GO30 and GO30-S30 removed CIP by 60.3 % and 60%, respectively, of their initial concentration, and the insignificant difference between the CIP removal efficiency could be negligible. The similar CIP adsorption trend shown over the 3 hours of testing on both samples suggested that the sonication step in the GO synthesis procedure has not been advantageous to GO quality.

From an economic standpoint, the sonication step was eliminated from the primary method of GO synthesis in this research since it prolongs the synthesis duration and does not guarantee an increase in GO quality for contaminant adsorption. Therefore, the GO30-S30 sample was not employed in this study's subsequent research to examine the effect of GO adsorption on other types of pharmaceutical contaminants.

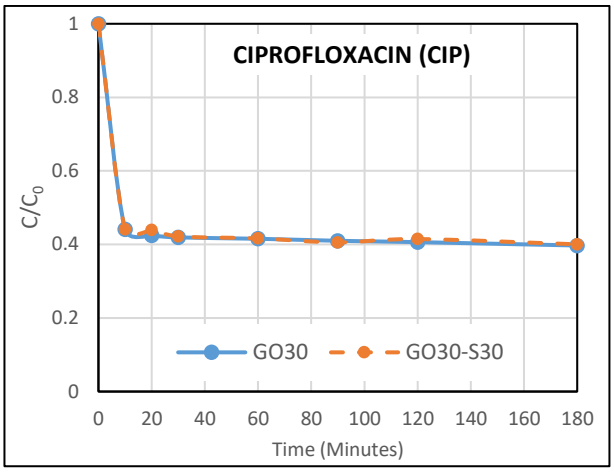

Fig. 3. Effect of sonication step on adsorption of CIP

3.4 The Kinetic Profile of GOs on the DCF Removal

The effect of GO synthesized by several methods on the adsorption of pharmaceutical contaminants was further investigated using the DCF antibiotic. Fig. 4 depicts the kinetics profile of all GO samples evaluated for DCF removal at different contact times for over 3 hours. Interestingly, GOM1 exhibited incredible adsorption capacity for this contaminant. The amount of DCF removed by this sample is more than that of the GOM3. GOM1 recorded a DCF removal efficiency of 94.3% at the first 10 minutes of contact time, while GOM3 recorded 73.2%. GOM1 was deemed to have reached absorption equilibrium at the 10th minute, even though no supporting catalyst was used to synthesize this sample. However, the GO30 and GO60 samples did not exhibit the expected performance during the 3-hour contact time, as shown in the CIP removal, because they only removed 57.1% and 61.7% of DCF from water, respectively. Again, this trend implies that the mixing periods in the GO synthesis optimized method have a negligible impact on the GO performance in removing DCF. The GOM2 sample shows the lowest DCF removal efficiency of 48.9%, besides its unstable absorption process shown.

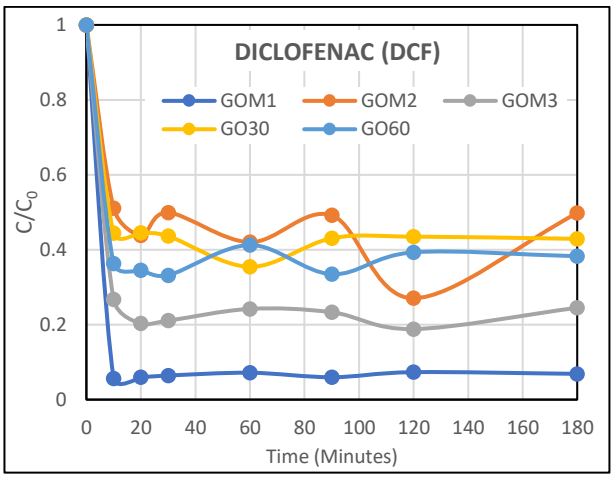

Fig. 4. Effect of contact time on adsorption of DCF

The outstanding removal efficiency shown by GOM1 may be ascribed to the presence of more numerous carboxyl functional groups on the surface [17]. The

longer oxidation process of 120 minutes and the high ratio of H2SO4 and an oxidizing agent (KMnO4) to graphite contributed to this functional group's formation behavior. This trend was consistent with the reduction in DCF removal performance presented by GOM3 when the oxidation process in synthesizing GO lasted 90 minutes. Lower DCF removal was shown by other samples when the oxidation period was only 20 minutes, and the ratio of the use of H_2SO_4 and the oxidizing agent to graphite was lower. Tran et al. [31] stated that GO functional groups, in addition to the sorption dynamic and surface area, have a significant role in the adsorption of DCF. Carboxylic groups of the GO's surface are more likely to interact with the carboxylic and amine groups of DCF than other functional groups to form stronger H-bonds [31]. Stemming from these findings, it is apparent that the production of high-quality GO for DCF removal does not rely on catalysts such as $NaNO_3$ or H_3PO_4.

3.5 The Kinetic Profile of GOs on the TC Removal

Fig. 5 shows the adsorption kinetics profile for TC removal within 3 hours of contact time for GO samples. Overall, the figure demonstrates that GO samples did not present reliable TC removal results since all the samples exhibited more petite than a 30% removal efficiency for TC with a 100 mg/L initial concentration within 3 hours of contact time. The TC removal efficiency was highest in the GOM2 sample, followed by the GOM1 sample, with 27.6% and 18.9% removal efficiency, respectively. While the GOM3, GO30, and GO60 samples did not show favorable TC adsorption when the removal efficiencies recorded were lower than 10% for 3 hours of contact time. Surprisingly, the GOM2 adsorption response mechanism seemed more stable in TC solution than in other pharmaceutical contaminants solutions. Based on these findings, the application of H3PO4 as a catalyst for converting graphite to GO contributed to the production of GO suitable for TC removal. According to Zou et al. [44], the inadequate electrostatic attraction interaction between the active surface area of GO and the TC might result in a relatively low GO adsorption capacity for this contaminant.

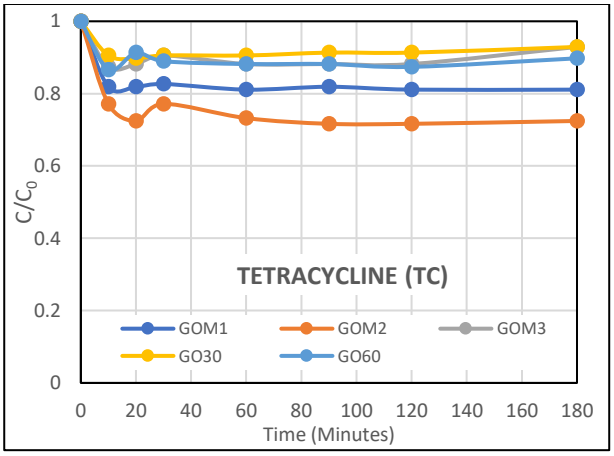

Fig. 5. Effect of contact time on adsorption of TC

4. CONCLUSION

Several GO synthesis methods on the performance of CIP, DCF, and TC removal from water were studied, and the synthesis method the GO was also optimized by compressing the time and optimizing the amount of raw material consumption. In a nutshell, the method of synthesizing GO with optimal time and materials used has successfully transformed graphite to GO, as evidenced by elemental composition analysis. GO synthesized with the optimized method showed the most reliable performance for the CIP removal from water, where 64% of CIP was effectively adsorbed within 10 minutes of contact time. The GOM1 sample showed the most maximal removal performance for DCF adsorption performance, where 94.3% of DCF was removed within 10 minutes of reaction. In addition, GOM2 is more likely to eliminate TC. GO synthesis methods play an essential role and have different effects on the removal of pharmaceutical contaminants. The performance of antibiotic removal (pharmaceutical contaminants) from water does not rely on catalysts, such as NaNO3 and H3PO4, particularly for CIP and DCF.

5. REFERENCES

[1] X. Qu, P. J. J. Alvarez, and Q. Li, “Applications of nanotechnology in water and wastewater treatment,” *Water Res.*, vol. 47, no. 12, pp. 3931–3946, 2013, doi: 10.1016/j.watres.2012.09.058.

[2] I. Maamoun, O. Eljamal, T. Shubair, H. Noutsuka, B. B. Saha, and N. Matsunaga, “Integrating nano-scale zero valent iron (nZVI) in phosphorus removal from aqueous solution through porous media: packed-column experiment,” *Proc. Int. Exch. Innov. Conf. Eng. Sci.*, vol. 3, pp. 25–30, 2017.

[3] I. Maamoun, O. Eljamal, O. Falyouna, R. Eljamal, and Y. Sugihara, “Multi-objective optimization of permeable reactive barrier design for Cr(VI) removal from groundwater,” *Ecotoxicol. Environ. Saf.*, vol. 200, no. April, p. 110773, 2020, doi: 10.1016/j.ecoenv.2020.110773.

[4] T. W. M. Amen, O. Eljamal, A. M. E. Khalil, and N. Matsunaga, “Wastewater degradation by iron/copper nanoparticles and the microorganism growth rate,” *J. Environ. Sci. (China)*, vol. 74, pp. 19–31, 2018, doi: 10.1016/j.jes.2018.01.028.

[5] “About | Thirst Relief.” https://thirstrelief.org/about/ (accessed Jul. 11, 2021).

[6] M. F. Idham, M. F. Masor, N. Mohd, B. Abdullah, and S. K. Alias, “Performance of Piper Nigrum (Black Pepper) as Corrosion Inhibitor of Ductile Iron,” vol. 7, pp. 115–118, 2018.

[7] I. Maamoun, R. Eljamal, O. Falyouna, K. Bensaida, Y. Sugihara, and O. Eljamal, “Insights into kinetics, isotherms and thermodynamics of phosphorus sorption onto nanoscale zero-valent iron,” *J. Mol. Liq.*, vol. 328, p. 115402, 2021, doi: 10.1016/j.molliq.2021.115402.

[8] X. Wang, R. Yin, L. Zeng, and M. Zhu, “A review of graphene-based nanomaterials for removal of antibiotics from aqueous environments,” *Environ. Pollut.*, vol. 253, pp. 100–110, 2019, doi: 10.1016/j.envpol.2019.06.067.

[9] O. Eljamal, J. Okawauchi, and K. Hiramatsu, “Removal of Phosphorus from Water Using Marble Dust as Sorbent Material,” *J. Environ. Prot. (Irvine,. Calif).*, vol. 03, no. 08, pp. 709–714, 2012, doi:

10.4236/jep.2012.38084.
[10] F. Y. Kong, Y. Luo, J. W. Zhang, J. Y. Wang, W. W. Li, and W. Wang, "Facile synthesis of reduced graphene oxide supported Pt-Pd nanocubes with enhanced electrocatalytic activity for chloramphenicol determination," *J. Electroanal. Chem.*, vol. 781, pp. 389–394, 2016, doi: 10.1016/j.jelechem.2016.06.018.
[11] Y. Yang, L. Xu, W. Li, W. Fan, S. Song, and J. Yang, "Adsorption and degradation of sulfadiazine over nanoscale zero-valent iron encapsulated in three-dimensional graphene network through oxygen-driven heterogeneous Fenton-like reactions," *Appl. Catal. B Environ.*, vol. 259, no. July, p. 118057, 2019, doi: 10.1016/j.apcatb.2019.118057.
[12] S. I. Siddiqui, P. N. Singh, N. Tara, S. Pal, S. A. Chaudhry, and I. Sinha, "Arsenic removal from water by starch functionalized maghemite nano-adsorbents: Thermodynamics and kinetics investigations," *Colloids Interface Sci. Commun.*, vol. 36, no. April, p. 100263, 2020, doi: 10.1016/j.colcom.2020.100263.
[13] Y. Hua *et al.*, "Effect of bicarbonate on aging and reactivity of nanoscale zerovalent iron (nZVI) toward uranium removal," *Chemosphere*, vol. 201, pp. 603–611, 2018, doi: 10.1016/j.chemosphere.2018.03.041.
[14] A. Chemistry, "Cinnamomum zeylanicum Extract as Green Corrosion Inhibitor for Carbon Steel in Hydrochloric Acid Solutions," *Prog. Chem. Biochem. Res.*, vol. 2, no. 3, pp. 120–133, 2019, doi: 10.33945/sami/pcbr.2019.2.5.
[15] O. Eljamal, J. Okawauchi, K. Hiramatsu, and M. Harada, "Phosphorus sorption from aqueous solution using natural materials," *Environ. Earth Sci.*, vol. 68, no. 3, pp. 859–863, 2013, doi: 10.1007/s12665-012-1789-6.
[16] A. Romero, M. P. Lavin-Lopez, L. Sanchez-Silva, J. L. Valverde, and A. Paton-Carrero, "Comparative study of different scalable routes to synthesize graphene oxide and reduced graphene oxide," *Mater. Chem. Phys.*, vol. 203, pp. 284–292, 2018, doi: 10.1016/j.matchemphys.2017.10.013.
[17] B. Y. Z. Hiew *et al.*, "Adsorptive decontamination of diclofenac by three-dimensional graphene-based adsorbent: Response surface methodology, adsorption equilibrium, kinetic and thermodynamic studies," *Environ. Res.*, vol. 168, no. September 2018, pp. 241–253, 2019, doi: 10.1016/j.envres.2018.09.030.
[18] S. Takami, O. Eljamal, A. M. E. Khalil, R. Eljamal, and N. Matsunaga, "Development of continuous system based on nanoscale zero valent iron particles for phosphorus removal," *J. Japan Soc. Civ. Eng.*, vol. 7, no. 1, pp. 30–42, 2019, doi: 10.2208/journalofjsce.7.1_30.
[19] T. Shubair, O. Eljamal, A. Tahara, Y. Sugihara, and N. Matsunaga, "Preparation of new magnetic zeolite nanocomposites for removal of strontium from polluted waters," *J. Mol. Liq.*, vol. 288, p. 111026, 2019, doi: 10.1016/j.molliq.2019.111026.
[20] N. A. Ahammad, M. A. Zulkifli, M. A. Ahmad, B. H. Hameed, and A. T. Mohd Din, "Desorption of chloramphenicol from ordered mesoporous carbon-alginate beads: Effects of operating parameters, and isotherm, kinetics, and regeneration studies," *J. Environ. Chem. Eng.*, vol. 9, no. 1, p. 105015, 2021, doi: 10.1016/j.jece.2020.105015.
[21] F. Aziz *et al.*, "Composites with alginate beads: A novel design of nano-adsorbents impregnation for large-scale continuous flow wastewater treatment pilots," *Saudi J. Biol. Sci.*, vol. 27, no. 10, pp. 2499–2508, 2020, doi: 10.1016/j.sjbs.2019.11.019.
[22] S. Wongcharee, V. Aravinthan, and L. Erdei, "Removal of natural organic matter and ammonia from dam water by enhanced coagulation combined with adsorption on powdered composite nano-adsorbent," *Environ. Technol. Innov.*, vol. 17, p. 100557, 2020, doi: 10.1016/j.eti.2019.100557.
[23] T. Zhang *et al.*, "Synergistic degradation of chloramphenicol by ultrasound-enhanced nanoscale zero-valent iron/persulfate treatment," *Sep. Purif. Technol.*, vol. 240, no. January, p. 116575, 2020, doi: 10.1016/j.seppur.2020.116575.
[24] O. Eljamal, T. Shubair, A. Tahara, Y. Sugihara, and N. Matsunaga, "Iron based nanoparticles-zeolite composites for the removal of cesium from aqueous solutions," *J. Mol. Liq.*, vol. 277, pp. 613–623, 2019, doi: 10.1016/j.molliq.2018.12.115.
[25] M. Selvakumar and S. Geetha, "Alkali activated porous material with nano graphene oxide as adsorbent in wastewater treatment," *Mater. Today Proc.*, vol. 45, pp. 4087–4090, 2019, doi: 10.1016/j.matpr.2021.04.198.
[26] I. Maamoun, O. Eljamal, R. Eljamal, O. Falyouna, and Y. Sugihara, "Promoting aqueous and transport characteristics of highly reactive nanoscale zero valent iron via different layered hydroxide coatings," *Appl. Surf. Sci.*, vol. 506, no. October 2019, p. 145018, 2020, doi: 10.1016/j.apsusc.2019.145018.
[27] G. Cui *et al.*, "Chitosan oligosaccharide derivatives as green corrosion inhibitors for P110 steel in a carbon-dioxide-saturated chloride solution," *Carbohydr. Polym.*, vol. 203, no. May 2018, pp. 386–395, 2019, doi: 10.1016/j.carbpol.2018.09.038.
[28] R. Eljamal, O. Eljamal, I. Maamoun, G. Yilmaz, and Y. Sugihara, "Enhancing the characteristics and reactivity of nZVI: Polymers effect and mechanisms," *J. Mol. Liq.*, vol. 315, p. 113714, 2020, doi: 10.1016/j.molliq.2020.113714.
[29] W. Peng, H. Li, Y. Liu, and S. Song, "A review on heavy metal ions adsorption from water by graphene oxide and its composites," *J. Mol. Liq.*, vol. 230, pp. 496–504, 2017, doi: 10.1016/j.molliq.2017.01.064.
[30] Y. Sun, Y. Yang, M. Yang, F. Yu, and J. Ma, "Response surface methodological evaluation and optimization for adsorption removal of ciprofloxacin onto graphene hydrogel," *J. Mol. Liq.*, vol. 284, pp. 124–130, 2019, doi: 10.1016/j.molliq.2019.03.118.
[31] T. Van Tran, D. T. C. Nguyen, H. T. N. Le, D. V. N. Vo, S. Nanda, and T. D. Nguyen, "Optimization, equilibrium, adsorption behavior and role of surface functional groups on graphene oxide-based nanocomposite towards diclofenac drug," *J. Environ. Sci. (China)*, vol. 93, pp. 137–150, 2020,

doi: 10.1016/j.jes.2020.02.007.
[32] J. Chen, G. M. He, G. Y. Xian, X. Q. Su, L. L. Yu, and F. Yao, "Mechanistic biosynthesis of SN-38 coated reduced graphene oxide sheets for photothermal treatment and care of patients with gastric cancer," *J. Photochem. Photobiol. B Biol.*, vol. 204, no. 2666, p. 111736, 2020, doi: 10.1016/j.jphotobiol.2019.111736.
[33] M. li Cao, Y. Li, H. Yin, and S. Shen, "Functionalized graphene nanosheets as absorbent for copper (II) removal from water," *Ecotoxicol. Environ. Saf.*, vol. 173, no. February, pp. 28–36, 2019, doi: 10.1016/j.ecoenv.2019.02.011.
[34] F. Tu, S. Liu, G. Jin, G. Yan, and C. Pan, "Fabrication of graphene from graphene oxide by ultrasonication with high Li storage capability," *Powder Technol.*, vol. 249, pp. 146–150, 2013, doi: 10.1016/j.powtec.2013.08.006.
[35] M. Sabzevari, D. E. Cree, and L. D. Wilson, "Graphene Oxide-Chitosan Composite Material for Treatment of a Model Dye Effluent," *ACS Omega*, vol. 3, no. 10, pp. 13045–13054, 2018, doi: 10.1021/acsomega.8b01871.
[36] M. Z. Kassaee, E. Motamedi, and M. Majdi, "Magnetic Fe3O4-graphene oxide/polystyrene: Fabrication and characterization of a promising nanocomposite," *Chem. Eng. J.*, vol. 172, no. 1, pp. 540–549, 2011, doi: 10.1016/j.cej.2011.05.093.
[37] Z. Chen *et al.*, "Performance of nitrogen-doped graphene aerogel particle electrodes for electro-catalytic oxidation of simulated Bisphenol A wastewaters," *J. Hazard. Mater.*, vol. 332, pp. 70–78, 2017, doi: 10.1016/j.jhazmat.2017.02.048.
[38] A. M. E. Khalil, F. A. Memon, T. A. Tabish, D. Salmon, S. Zhang, and D. Butler, "Nanostructured porous graphene for efficient removal of emerging contaminants (pharmaceuticals) from water," *Chem. Eng. J.*, vol. 398, no. May, p. 125440, 2020, doi: 10.1016/j.cej.2020.125440.
[39] H. Chen, B. Gao, and H. Li, "Removal of sulfamethoxazole and ciprofloxacin from aqueous solutions by graphene oxide," *J. Hazard. Mater.*, vol. 282, pp. 201–207, 2015, doi: 10.1016/j.jhazmat.2014.03.063.
[40] J. Xu, X. Liu, Z. Cao, W. Bai, Q. Shi, and Y. Yang, "Fast degradation, large capacity, and high electron efficiency of chloramphenicol removal by different carbon-supported nanoscale zerovalent iron," *J. Hazard. Mater.*, vol. 384, no. September 2019, p. 121253, 2020, doi: 10.1016/j.jhazmat.2019.121253.
[41] M. J. Yoo and H. B. Park, "Effect of hydrogen peroxide on properties of graphene oxide in Hummers method," *Carbon N. Y.*, vol. 141, pp. 515–522, 2019, doi: 10.1016/j.carbon.2018.10.009.
[42] A. Arabpour, S. Dan, and H. Hashemipour, "Preparation and optimization of novel graphene oxide and adsorption isotherm study of methylene blue," *Arab. J. Chem.*, vol. 14, no. 3, p. 103003, Mar. 2021, doi: 10.1016/j.arabjc.2021.103003.
[43] L. Han *et al.*, "Graphene oxide-induced formation of a boron-doped iron oxide shell on the surface of NZVI for enhancing nitrate removal," *Chemosphere*, vol. 252, 2020, doi: 10.1016/j.chemosphere.2020.126496.
[44] S. J. Zou, Y. F. Chen, Y. Zhang, X. F. Wang, N. You, and H. T. Fan, "A hybrid sorbent of α-iron oxide/reduced graphene oxide: Studies for adsorptive removal of tetracycline antibiotics," *J. Alloys Compd.*, vol. 863, p. 158475, 2021, doi: 10.1016/j.jallcom.2020.158475.